

THE NUCLEAR QUADRUPOLE COUPLING TENSORS OF  $\text{Al}^{27}$  IN KYANITESTEFAN HAFNER AND MICHAEL RAYMOND, *Department of the Geophysical Sciences, University of Chicago, Chicago, Illinois.*

## ABSTRACT

The nuclear electric quadrupole coupling tensors of  $\text{Al}^{27}$  at the four nonequivalent aluminum sites in kyanite have been determined by use of nuclear magnetic resonance. The eigenvalues and the asymmetry parameters  $\eta$  are: 10.0 MHz, 9.4 MHz, 6.5 Hz, 3.7 MHz, and 0.27, 0.38, 0.59, 0.89, respectively. The magnitudes of two of the coupling tensors are the greatest found to date in any aluminum compound. Each of the four tensors indicates a strong electronic polarization of the aluminum atoms approximately parallel to *b*.

The external electric field gradient tensors at the aluminum sites have been calculated by the ionic point charge model. While there is a coarse agreement between the observed and calculated eigenvectors of the tensors, the eigenvalues do not agree. Especially the two largest eigenvalues cannot be explained by this model.

## INTRODUCTION

Nuclear quadrupole coupling tensors of atoms in crystals are very sensitive parameters of the actual electron density distribution in the crystal structure. They are a measure of the slight electronic deformation of the atoms at their sites caused by the net charges of the neighboring atoms (ionic polarization) and by bonding. In this paper, the quadrupole coupling tensors of  $\text{Al}^{27}$  in kyanite are reported. The crystal structure of kyanite is particularly appropriate, and we will present a brief discussion of the  $\text{Al}^{27}$  tensors of this mineral, although definite conclusions are not as yet possible.

The nuclear electric quadrupole interaction of an atom which possesses a free ionic state with noble gas configuration such as  $\text{Al}^{+3}$  is usually written as

$$eQV_{ij} = eQ(1 - \gamma_{\infty})V_{ij}^{\text{ext}} \quad (1)$$

$Q$  in equation (1) is the nuclear quadrupole moment,  $V_{ij}$  is the electric field gradient tensor at the nucleus which is a second rank tensor with vanishing trace,  $\gamma_{\infty}$  is the polarization factor of Sternheimer, and  $V_{ij}^{\text{ext}}$  is the electric field gradient tensor at the atomic position due to the net charges of the neighboring ions.  $Q$  of  $\text{Al}^{27}$  is known ( $0.149 \times 10^{-24}$  cm<sup>2</sup>).  $\gamma_{\infty}$  has been calculated theoretically for the free  $\text{Al}^{+3}$  ion (Das and Bersohn, 1956; Burns, 1959).

The symmetry properties of the field gradient tensors  $V_{ij}$  and  $V_{ij}^{\text{ext}}$  are determined by the point symmetry of the atomic position. If the position possesses a cubic point symmetry the tensors will vanish. However, if the point symmetry is lower than cubic a permanent field gradient at the

nucleus will be induced by  $V_{ij}^{\text{ext}}$  and a definite quadrupole interaction will occur.  $V_{ij}^{\text{ext}}$  can be derived from the crystal structure by using the ionic model. If the nuclear quadrupole coupling tensors  $eQV_{ij}$  are determined experimentally the Sternheimer factor  $\gamma_\infty$  and  $V_{ij}^{\text{ext}}$  can be tested by means of equation (1).

Kyanite is a particularly favourable case for such a test. Its structure has the relatively high number of four non-equivalent aluminum sites with low point symmetries ( $C_1$ ) in a relatively small unit cell which contains only three different atoms and only four formula units  $\text{Al}_2\text{SiO}_6$ . Since the quadrupole coupling tensors at the four Al sites are not reduced by any symmetry elements they are each described by five independent

TABLE 1. TRANSFORMATION MATRIX FROM TRICLINIC TO ORTHOGONAL AXES FOR KYANITE

	$x'$	$y'$	$z'$
$a$	0.9418	-0.2757	-0.1925
$b$	0	1	0
$c$	0	0.0004	1.0000

parameters. Therefore, the four tensor equations (1) consist of 20 linear equations with 20 experimentally determined independent parameters.

Since silicates such as kyanite are resonance structures which cannot be fully accounted for by the ionic model discussion of equation (1) and a test of its adequacy will be interesting.

#### EXPERIMENTAL

The four quadrupole coupling tensors of  $\text{Al}^{27}$  have been measured by nuclear magnetic resonance. For this, we have used the perturbation theory approach in which the nuclear magnetic energy levels are perturbed by the nuclear electric quadrupole interaction.<sup>1</sup> A single crystal from Brazil was cut to a cubic shape with an edge length of about 10 mm. Resonance was observed at a fixed frequency of 11 MHz by sweeping the magnetic field from about 8 to 12 kilogauss. The homogeneity of the field was higher than necessary ( $\sim 10^{-7}$  within the volume of the crystal). The field was repeatedly calibrated with the resonance line of an Al aqueous solution. The resonance signals of the crystal were exceedingly strong and relatively sharp with a half width of about 5 gauss. A typical resonance spectrum is given in Figure 1.

The quadrupole coupling tensors can be accurately determined under such conditions. Misalignment of the crystallographic axes with respect to the magnetic field is the largest source of error. The accuracy is hence mainly determined by the goniometer facilities avail-

<sup>1</sup> For a detailed description of the technique the reader is referred to the articles of Pound (1950) and Volkoff *et al.* (1953).

able for the resonance experiment. For our investigation we did not attempt to align the crystal more precisely than about  $\pm$  one degree, although an error of one degree may lead to line shifts of more than 30 gauss in extreme cases, while the lines can be measured with a precision of  $\pm$  one gauss or better. The crystal was oriented with the back-reflection method of Laue.

It is convenient to represent the tensors in an orthogonal crystal system  $x'$ ,  $y'$ ,  $z'$ . For this, we have chosen  $y'$  parallel to the  $b$ -axis, and  $z'$  in the  $b$ - $c$  plane, as shown in Figure 3. The matrix for the coordinate transformation from the triclinic system  $a$ ,  $b$ ,  $c$  to the system  $x'$ ,  $y'$ ,  $z'$  is given in Table 2. The crystal was rotated around an axis perpendicular to the magnetic field. Spectra were taken every 7.5 degrees. Three rotations were performed with  $x'$ ,  $y'$ , and  $z'$ , respectively, parallel to the axis of rotation.

The angular dependence of the differences  $\Delta$  of the *inner* pair of satellite signals ( $m = -3/2 \rightarrow -1/2$ ,  $m = 1/2 \rightarrow 3/2$ ) was used for determining the parameters  $A_i$ ,  $B_i$ , and  $C_i$  of the three rotations. If the terms of third and higher order of perturbation theory are neglected the dependence of  $\Delta(\theta)$  on  $A_i$ ,  $B_i$ , and  $C_i$  is simply

$$\Delta(\theta) = A_i + B_i \cos 2\theta + C_i \sin 2\theta_j \quad i = x', y', z' \quad (2)$$

$\theta$  in equation (2) is the rotation angle.  $A_i$ ,  $B_i$ , and  $C_i$  were found by fitting  $\Delta$  to the data of each of the three rotations and by use of the five identities

$$\begin{aligned} A_{x'} + A_{y'} + A_{z'} &= 0 \\ B_{x'} + B_{y'} + B_{z'} &= 0 \\ A_{y'} + B_{y'} &= A_{x'} - B_{x'}; \text{ etc.} \end{aligned}$$

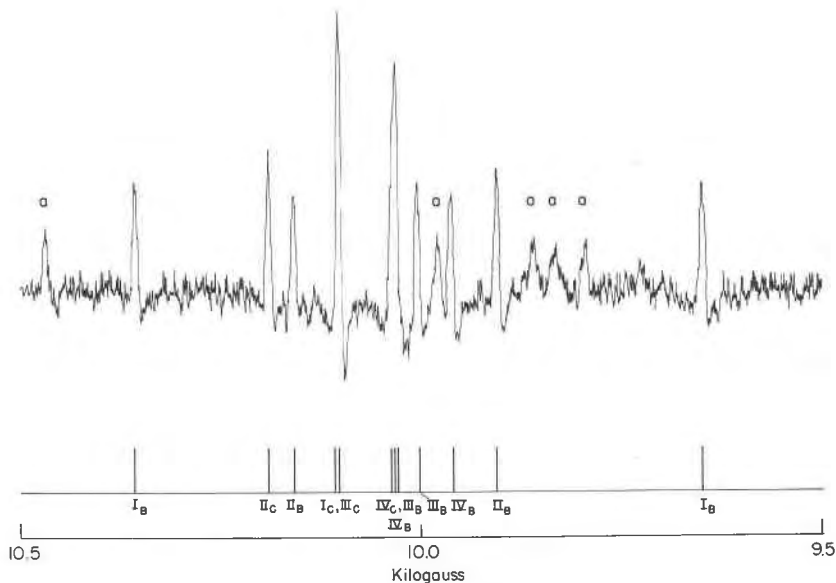


FIG. 1. Resonance spectrum of kyanite.  $z'$  is perpendicular to the magnetic field. The angle  $\theta$  between  $x'$  and the magnetic field is  $45^\circ$ . The numbers I, II, III, IV refer to the tensor numbers (Table 3). The subscripts C and B indicate central signals and inner satellites, respectively. a: outer satellites. Dispersion mode signals.

The  $A_i$  and  $B_i$  values were weighted according to their precision and averaged. It is possible to derive  $C_i$  also from the angular dependence of the central signals, although conditions of accuracy did not permit this in our experiment.

The quadrupole coupling tensors are finally given by the relations

$$eQV_{x'x'} = -2kA_{x'} \tag{3}$$

$$eQV_{y'y'} = k(A_{x'} + B_{x'}) \tag{4}$$

$$eQV_{z'z'} = k(A_{x'} - B_{x'}) \tag{5}$$

$$eQV_{y'z'} = -kC_{x'}; \text{ etc.} \tag{6}$$

$$k = \frac{2I(2I - 1)\gamma\hbar}{6} \tag{7}$$

$I$  in equation (7) is the nuclear spin (5/2 for  $\text{Al}^{27}$ ) and  $\gamma$  is the gyromagnetic ratio ( $\gamma$  of  $\text{Al}^{27} = 6.9706 \text{ MHz /kilogauss}$ ).

TABLE 2.  $A_i$ ,  $B_i$ , AND  $C_i$  PARAMETERS OF KYANITE

Tensor	$x'$ rotation kilogauss		$y'$ rotation kilogauss		$z'$ rotation kilogauss	
I	$A_{x'}$	0.523	$A_{y'}$	-1.239	$A_{z'}$	0.714
	$B_{x'}$	1.965	$B_{y'}$	-0.207	$B_{z'}$	-1.771
	$C_{x'}$	0.992	$C_{y'}$	-0.186	$C_{z'}$	-0.015
II	$A_{x'}$	0.879	$A_{y'}$	-1.244	$A_{z'}$	0.370
	$B_{x'}$	1.641	$B_{y'}$	0.496	$B_{z'}$	-2.145
	$C_{x'}$	-0.379	$C_{y'}$	-0.054	$C_{z'}$	-0.108
III	$A_{x'}$	0.679	$A_{y'}$	-0.831	$A_{z'}$	0.155
	$B_{x'}$	0.993	$B_{y'}$	0.522	$B_{z'}$	-1.513
	$C_{x'}$	-0.442	$C_{y'}$	-0.232	$C_{z'}$	-0.117
IV	$A_{x'}$	0.422	$A_{y'}$	-0.463	$A_{z'}$	0.043
	$B_{x'}$	0.503	$B_{y'}$	0.377	$B_{z'}$	-0.892
	$C_{x'}$	0.281	$C_{y'}$	0.294	$C_{z'}$	0.018

RESULTS

The parameters  $A_i$ ,  $B_i$ , and  $C_i$  are listed in Table 2. The dimension of the parameters is kilogauss since we found it more convenient to sweep the magnetic field than the frequency. Table 3 presents the eigenvalues of the diagonalized tensors and the eigenvectors with respect to the  $x'$ ,  $y'$ , and  $z'$  system. Two of the tensors have extremely great eigenvalues. This is manifested by the extraordinary splitting of the satellite resonance lines by several kilogauss at 11 MHz. The central signals which depend on second- and higher- order effects only are shifted by several hundred gauss.

We have used the final quadrupole coupling tensors to calculate all the

line positions as a function of  $\theta$  for each of the three rotations, using perturbation theory. The third-order terms have been included. They were found to average about 20 gauss, the greatest contribution being 60 gauss for tensor II ( $z'$  rotation,  $\theta = 30^\circ$ ). The third-order effects are thus substantial. They can be well resolved in the spectrum. Therefore, equation (2) yields only approximate values for the tensors. However, the third order effects are still of the order of the errors of alignment of the crystal with respect to the magnetic field. The maximum deviation of the calcu-

TABLE 3. MEASURED NUCLEAR QUADRUPOLE COUPLING TENSORS OF  $\text{Al}^{27}$  IN KYANITE

Tensor	Eigenvalues <sup>a</sup> $eQV_{ii}/h$ , MHz	Eigenvectors (Direction Cosines)			
		$x'$	$y'$	$z'$	
I	$i=x$	$\mp 3.68 \pm 0.07$	$0.964 \pm 0.010$	$0.069 \pm 0.007$	$0.256 \pm 0.013$
	$i=y$	$\mp 6.34 \pm 0.13$	$-0.265 \pm 0.014$	$0.223 \pm 0.012$	$0.938 \pm 0.013$
	$i=z$	$\pm 10.04 \pm 0.20$	$0.008 \pm 0.020$	$-0.972 \pm 0.011$	$0.233 \pm 0.033$
II	$i=x$	$\mp 2.89 \pm 0.04$	$0.042 \pm 0.007$	$-0.116 \pm 0.006$	$0.992 \pm 0.004$
	$i=y$	$\mp 6.52 \pm 0.10$	$-0.999 \pm 0.003$	$0.021 \pm 0.011$	$0.045 \pm 0.025$
	$i=z$	$\pm 9.37 \pm 0.14$	$0.026 \pm 0.020$	$0.993 \pm 0.005$	$0.115 \pm 0.034$
III	$i=x$	$\mp 1.35 \pm 0.03$	$0.197 \pm 0.007$	$-0.220 \pm 0.005$	$0.955 \pm 0.011$
	$i=y$	$\mp 5.20 \pm 0.09$	$-0.979 \pm 0.016$	$0.008 \pm 0.014$	$0.204 \pm 0.030$
	$i=z$	$\pm 6.53 \pm 0.12$	$0.052 \pm 0.025$	$0.976 \pm 0.013$	$0.213 \pm 0.037$
IV	$i=x$	$\mp 0.20 \pm 0.01$	$-0.342 \pm 0.006$	$0.253 \pm 0.009$	$0.905 \pm 0.012$
	$i=y$	$\mp 3.52 \pm 0.07$	$0.939 \pm 0.020$	$0.060 \pm 0.023$	$0.339 \pm 0.029$
	$y=z$	$\pm 3.70 \pm 0.07$	$-0.032 \pm 0.028$	$-0.966 \pm 0.012$	$0.258 \pm 0.031$

<sup>a</sup> The sign of the eigenvalues cannot be determined experimentally.

lated *central signal* positions from the observed lines was 10 gauss. From this, we conclude that the quadrupole coupling tensors should be correct within the limits of error marked in Table 3, although the third-order effects have been neglected. A refined determination of the tensors should nevertheless take them into account. It would also be interesting to re-examine the tensors by means of pure quadrupole resonance.

#### DISCUSSION

In Table 4, the  $\text{Al}^{27}$  quadrupole coupling tensors of kyanite are compared with those of a number of aluminum oxides and aluminum silicates. The four kyanite tensors are surprisingly distinct. Two of them are by far the greatest observed to date in any aluminum compound. The two

others are considerably smaller. The quadrupole energy difference of more than 6 MHz between the smallest and the greatest value is unusually large for  $Al^{27}$  tensors of nonequivalent sites with the same number of nearest neighboring atoms. Such marked differences of the tensor properties must be attributed to distinct crystallographical properties of the corresponding sites.

The crystal structure of kyanite was determined by Naray-Szabo,

TABLE 4. THE NUCLEAR QUADRUPOLE COUPLING TENSORS OF  $Al^{27}$  IN SOME ALUMINUM OXIDES AND ALUMINUM SILICATES (MAXIMUM EIGEN VALUES AND ASYMMETRY PARAMETERS  $\eta$ )

	$eQV_{zz}/h$ MHz	Al-site	$\eta$	Reference
A. Oxides				
1. Corundum ( $Al_2O_3$ )	2.393	octahedral	0	Pound (1950)
2. Chrysoberyl ( $BeAl_2O_4$ )	2.850	octahedral	0.94	Hockenberry (1958)
	2.846	octahedral	0.76	
3. Spinel ( $MgAl_2O_4$ )	3.68	octahedral	0	Brun (1952)
4. Lithium Aluminate ( $LiAl_2O_4$ )	0.284	tetrahedral	0	Stauss (1964)
	0.683	octahedral	0.347	
5. Berlinite ( $AlPO_4$ )	4.088	tetrahedral	0.367	Brun (1961)
B. Silicates				
6. Natrolite ( $Na_2Al_2Si_3O_{10} \cdot 2H_2O$ )	1.663	tetrahedral	0.5029	Petch (1962)
7. Euclase ( $HBeAlSiO_5$ )	5.173	octahedral	0.698	Eades (1955)
8. Beryl ( $Be_3Al_2(SiO_3)_6$ )	3.093	octahedral	0	Brown (1956)
9. Spodumene ( $LiAl(SiO_3)_2$ )	2.950	octahedral	0.94	Petch (1953)
10. Albite ( $NaAlSi_3O_8$ )	3.29	tetrahedral	0.26	Hartmann (1963)
11. Microcline ( $KAlSi_3O_8$ )	3.21	tetrahedral	0.21	Hartmann (1963)
	10.04	octahedral	0.27	
	9.37	octahedral	0.38	
	6.53	octahedral	0.59	
12. Kyanite ( $Al_2SiO_5$ )	6.53	octahedral	0.59	This work
	3.70	octahedral	0.89	

Taylor, and Jackson (1929). A refinement of the atomic coordinates was performed by Burnham (1963)<sup>1</sup>. The structure is described as a distorted cubic close-packed arrangement of oxygen atoms in which the aluminum atoms are located in certain octahedral interstices while silicon occurs in certain tetrahedral interstices. The distribution of aluminum among the octahedral interstices is such that one half of the Al-O octahedra, Al(1) and Al(2), form chains parallel to the  $c$  axis, successive octahedra sharing edges. The other half of the aluminum octahedra, Al(3) and Al(4), link the chains together in that they share edges with the chain octahedra.

<sup>1</sup> Another refinement of kyanite was performed by de Rango *et al.*, (1966).

The Al(1) and Al(3) octahedra each share five edges with neighboring aluminum octahedra while Al(2) and Al(4) each have four edges with other octahedra in common. Thus, each of the four Al sites is topologically distinct:

- Al(1) octahedron of a chain parallel to  $c$ , five edges shared
- Al(2) octahedron of a chain parallel to  $c$ , four edges shared
- Al(3) not in a chain, five edges shared
- Al(4) not in a chain, four edges shared

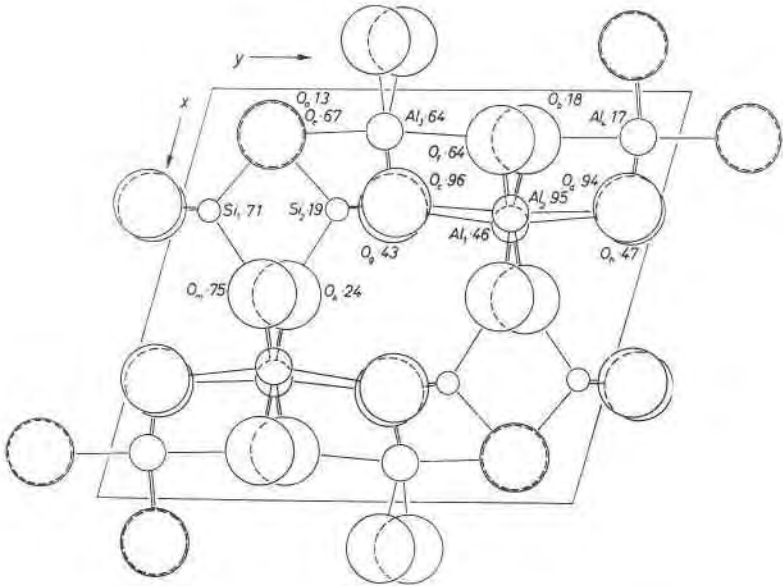


FIG. 2. Projection of the kyanite structure parallel to  $c$ . Reproduction of Fig. 2 of Burnham (1963).

It would be interesting to know the assignment of the four tensors I, II, III, and IV to the four Al sites. However, since the point symmetry of all four sites is the same ( $C_1$ ), the tensors cannot be assigned simply by symmetry considerations and inspection of the spectra. Burnham (1963) found that the Al(4) octahedron is strongly distorted, possessing the shortest and one of the longest Al-O distances observed in aluminum silicate minerals. Its assignment to one of the tensors with the large eigenvalues is therefore probable, although by no means definite.

Second rank tensors with vanishing trace are represented geometrically by three axial hyperboloids. The eigenvectors describe the directions of

the hyperboloidal symmetry axes and the eigenvalues give their axial lengths. The eigenvectors of the four measured  $\text{Al}^{27}$  tensors are shown in Figure 3. For each tensor, one symmetry axis is nearly parallel to the  $b$  direction of the crystal, and another is nearly parallel to  $c$ . In each case the symmetry axes parallel to  $b$  are in the direction of the greatest electric field gradient. Thus, all the aluminum atoms are strongly polarized in

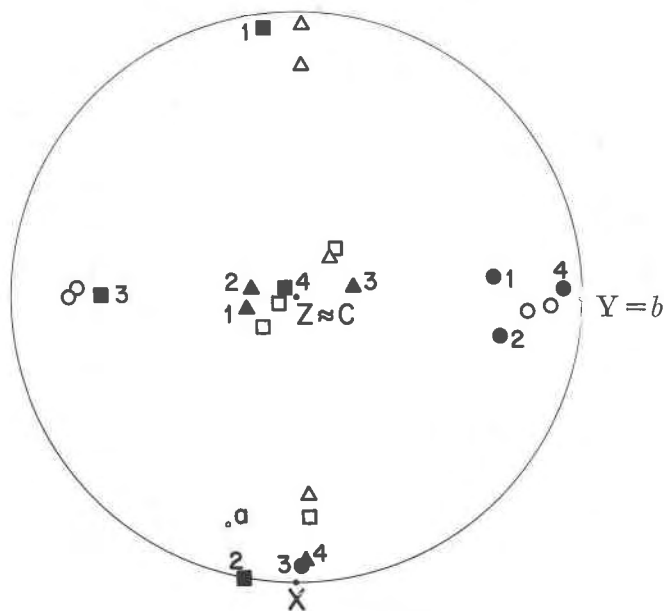


FIG. 3. Stereographic projection of the observed and calculated eigenvectors of the nuclear quadrupole tensors. Circles:  $V_{zz}$ , triangles:  $V_{yy}$ , squares:  $V_{xx}$ . Open symbols: observed vectors; solid symbols: calculated vectors. The numbers of the solid symbols refer to the subscripts of the Al sites.

that direction. The  $b$ -direction is in fact a special direction of all Al-O octahedra in the kyanite crystal structure, (Fig. 2).

Using the point charge model, we have calculated the electric field gradient tensors  $V_{ij}^P$  at the four aluminum sites. For this the Ewald lattice potentials at the sites were expanded in spherical harmonics (the gradients can be computed very accurately by this technique). The atomic coordinates of the refinement of Burnham were used<sup>1</sup>. The eigenvalues and eigenvectors are listed in Table 5; the latter are also shown in

<sup>1</sup> We have repeated the computations using the atomic coordinates of de Rango *et al.*, (1966). Although there are differences in the results due to the slightly different coordinates, the conclusions are not affected.



TABLE 5. CALCULATED ELECTRIC FIELD GRADIENTS AT THE Al SITES IN KYANITE (POINT CHARGE MODEL)

Site	Eigenvalues		Eigenvectors (Direction Cosines)		
			$x'$	$y'$	$z'$
Al <sub>1</sub>	$V_{xx}$	-0.32	-0.991	-0.127	0.045
	$V_{yy}$	-2.10	0.086	-0.343	0.935
	$V_{zz}$	+2.43	-0.104	0.931	0.351
Al <sub>2</sub>	$V_{xx}$	+0.40	0.984	-0.178	0.005
	$V_{yy}$	+1.79	-0.061	-0.310	0.949
	$V_{zz}$	-2.19	0.167	0.934	0.316
Al <sub>3</sub>	$V_{xx}$	-0.83	-0.002	-0.928	0.372
	$V_{yy}$	-1.21	-0.076	0.371	0.926
	$V_{zz}$	+2.03	0.997	0.026	0.072
Al <sub>4</sub>	$V_{xx}$	+0.16	-0.073	-0.073	0.995
	$V_{yy}$	+2.39	0.996	0.031	0.077
	$V_{zz}$	-2.56	-0.046	0.996	0.070

Figure 3. In Table 6, the maximum eigenvalues and asymmetry parameters  $\eta$  of the quadrupole coupling tensors calculated by use of equation (1) are given. For the calculation, the theoretical value  $\gamma_\infty = -2.45$  of the free Al<sup>3+</sup> ion was taken. Further, it was assumed that

$$V_{ij}^{\text{ext}} \approx V_{ij}^P. \quad (8)$$

The agreement between the observed and the calculated eigenvalues of the quadrupole coupling tensors is far from being satisfactory in spite of the fact that there is coarse coincidence between the eigenvectors. Although it is reasonable to expect that the computed field gradient tensor

TABLE 6. OBSERVED AND CALCULATED MAXIMUM EIGENVALUES OF THE Al<sup>27</sup> QUADRUPOLE COUPLING TENSORS

Measured		Calculated		
$eQV_{zz}/h, \text{MHz}$	$\eta$	$(1-\gamma_a)eQV_{zz}^P/h$ $\text{MHz}$	$\eta$	Site
$10.04 \pm 0.20$	$0.27 \pm 0.02$	-2.56	0.87	Al (4)
$9.37 \pm 0.14$	$0.38 \pm 0.01$	+2.43	0.73	Al (1)
$6.53 \pm 0.12$	$0.59 \pm 0.02$	-2.19	6.63	Al (2)
$3.70 \pm 0.07$	$0.89 \pm 0.02$	+2.03	0.19	Al (3)

at the Al(4) site is the greatest of the four (see Table 4), the four tensors are roughly equal, and the unique values of the tensors I and II cannot be interpreted by the simple point charge model. Two of the symmetry axes of the calculated tensors are more or less parallel to the  $b$  and  $c$  directions of the crystal, in agreement with the experimental results outlined above. The symmetry axes parallel to  $b$  are, with one exception, again the directions of the greatest field gradient. It is to be noted that the eigenvectors are fully determined with respect to the crystallographic axes  $a$ ,  $b$ ,  $c$  of the crystal. There is no freedom for any rotation. The direction of the vectors together with  $a$ ,  $b$ ,  $c$  is plotted in Figure 3.

Two possibilities may explain the discrepancy between observed and calculated eigenvalues: first, the point charge model is generally inadequate for the calculation of ionic field gradients at lattice sites. The higher electronic moments of the ions contribute considerably to the effective gradients  $V_{ij}^{\text{ext}}$ . Their contribution is of the same order of magnitude as the point charge contribution alone, particularly in crystal structures with low lattice symmetry. Secondly, the purely ionic model is probably not very accurate for resonance structures such as silicates. However, it must be remembered that any nonionic contribution to the quadrupole tensors can be determined only when the electric field gradients of the ideal ionic model are known. Therefore, self-consistent calculations of the ionic field gradients, including the higher electronic moments of the ions, are necessary. Unfortunately, such computations for kyanite are lengthy, due to the relatively high number of nonequivalent atomic positions and their low point symmetries. A detailed investigation of the higher electronic moments in kyanite is under way.

This work was supported by the National Science Foundation under Grant GP-5097. The experiments were performed at the Institute for the Study of Metals at the University of Chicago.

#### REFERENCES

- BROWN, L. C. AND D. WILLIAMS (1956) Quadrupolar splitting of the Al<sup>27</sup> and Be<sup>9</sup> magnetic resonances in beryl crystals. *J. Chem. Phys.* **24**, 751-756.
- BRUN, E. AND S. HAFNER (1962) Die Elektrische Quadrupolspaltung von Al<sup>27</sup> in Spinell MgAl<sub>2</sub>O<sub>4</sub> und Korund Al<sub>2</sub>O<sub>3</sub>. *Z. Kristallogr.* **117**, 37-62.
- , P. HARTMANN, F. LAVES AND D. SCHWARZENBACH (1961) Elektrische Quadrupolwechselwirkung von Al<sup>27</sup> in AlPO<sub>4</sub>. *C. R. Acad. Sci. Paris* **34**, 388-391.
- BURNHAM, C. W. (1963) Refinement of the crystal structure of kyanite. *Z. Kristallogr.* **118**, 337-360.
- BURNS, G. (1959) Polarizabilities and antishielding factors of 10 and 18 electron closed shell atoms. *J. Chem. Phys.* **31**, 1253-1255.
- DAS, T. P. AND R. BERSOHN (1956) Variational approach to the quadrupole polarizability of ions. *Phys. Rev.* **102**, 733-738.
- EADES, R. G. (1955) An investigation of the nuclear resonance absorption spectrum of Al<sup>27</sup> in a single crystal of euclase. *Can. J. Phys.* **33**, 286-297.

- HARTMANN, P. (1963) *Untersuchungen von Quadrupoleffekten in Kernresonanzspektren von Feldspäten*. Diss. Univ. Zurich, Switzerland.
- HOCKENBERRY, J. H., JR., L. C. BROWN AND D. WILLIAMS (1958) Nuclear resonance spectrum of  $Al^{27}$  in chrysoberyl. *J. Chem. Phys.* **28**, 367-372.
- NARAY-SZABO, S., W. H. TAYLOR AND W. W. JACKSON (1929) The structure of cyanite. *Z. Kristallogr.* **71**, 117-130.
- PETCH, H. E., N. G. CRANNA AND G. M. VOLKOFF (1953) Second order nuclear quadrupole effects in single crystals. Part II. Experimental results for spodumene. *Can. J. Phys.* **31**, 837-858.
- AND K. S. PENNINGTON (1962) Nuclear quadrupole coupling tensors for  $Na^{23}$  and  $Al^{27}$  in natrolite, a fibrous zeolite. *J. Chem. Phys.* **36**, 1216-1221.
- POUND, R. V. (1950) Nuclear electric quadrupole interactions in crystals. *Phys. Rev.* **79**, 685-702.
- RANGO DE, C., G. TSOUKARIS, C. ZELWER AND J. DEVAUX (1966) Comparaison de deux affinements de la structure de la cyanite. *Bull. Soc. Franç. Mineral. Cristallogr.* **89**, 419-424.
- STAUSS, G. H. (1964) Nuclear magnetic resonance determination of some microscopic parameters of  $LiAl_5O_8$ . *J. Chem. Phys.* **40**, 1988-1991.
- VOLKOFF, G. M. (1953) Second order nuclear quadrupole effects in single crystals. Part I. Theoretical. *Can. J. Phys.* **31**, 820-836.

*Manuscript received, April 10, 1967; accepted for publication, July 3, 1967.*